Recent Advances in Real-Time Load-Pull Systems

Valeria Teppati, *Member, IEEE*, Andrea Ferrero, *Member, IEEE*, and Umberto Pisani

***Abstract*—In this paper, some of the latest advances in real-time load-pull technologies will be described. A recently introduced ultralow-loss directional coupler, which has been designed and realized by the authors, provides a number of advantages when used in load-pull test sets. This device has been called the *load-pull head*. The new ultralow-loss load-pull head can transform any passive precalibrated load-pull system into an easily calibrated and accurate real-time load-pull test set, without losing high-reflection-coefficient capabilities. Moreover, if used to realize an active loop, the load-pull head reduces the risks of oscillations and the amount of the loop amplifier output power. As an example application, measurements with a passive real-time load-pull setup of a 30-W laterally diffused MOS (LDMOS) transistor are presented. Furthermore, some advice to bypass the remaining unavoidable losses due to probes and cables is given. We will show, with measurements and with very simple calculations, that the combined use of load-pull heads, a passive tuner, and an active loop not only boosts the available Γ_L but also decreases the loop amplifier output power, with a sensible reduction in the overall cost of the system.**

***Index Terms*—Directional couplers, microwave devices, microwave measurements, microwave phase shifters, microwave power amplifiers, microwave power FETs, tuners, yttrium iron garnet filters.**

I. Introduction

LOAD-PULL measurements monitor the nonlinear performances of a device under test (DUT) while driving it with different load impedance values. They are a powerful tool to characterize and extract models of active devices, as well as to design and verify nonlinear circuits such as power amplifiers, mixers, etc. [1], [2]. Modern load-pull systems can be classified into two main typologies, shown in Fig. 1: 1) real-time systems [Fig. 1(a)] and 2) nonreal-time systems [Fig. 1(b)].

The real-time load-pull scheme is derived from the classical scattering parameter (S-parameter) test set, with high-power couplers and external attenuators (for simplicity, these are not shown in figure) on the couplers' arms. The raw measurements a_{m1}, b_{m1}, a_{m2}, and b_{m2} are referred to the DUT planes with the classical calibration procedures for two-port systems [3]–[6]. Moreover, absolute power levels at the reference planes are calculated with some additional standards and a power meter connected to a coaxial port during the calibration phase [7]–[10].

From the knowledge of the corrected input and output waves a_1, b_1, a_2, and b_2 at DUT reference planes, all the performances of interest (e.g., reflection coefficients, power, and gain) are computed. These systems directly inherit from the vector network analyzer (VNA) all the characteristics of high-speed, high-accuracy, fast, and flexible calibration procedures.

The main drawback of these systems consists of the losses of the directional couplers, which prevent the highest reflection coefficients from being reached if passive tuners are used. For this reason, real-time systems are generally coupled with active loads, whereas passive tuners are used in the nonreal-time configuration in Fig. 1(b), i.e., placed as close as possible to the DUT.

With the latter architecture, it is not possible to perform a single VNA calibration, as in real-time systems, because the variable loads are placed in the path between the reflectometers and the DUT reference planes; see Fig. 1(b). To have corrected measurements at the DUT reference planes, the S-parameters of each system component and of the tuners, for each tuner position, must be measured during a precharacterization phase. The accuracy of the load-pull measurements will then rely on the tuner and connector repeatability. Moreover, precharacterization is a time-consuming procedure, if compared with the real-time load-pull system calibration.

This drawback can be overcome by using the new ultralow-loss broadband high-power directional couplers designed and realized by the authors and described in Section II. The new couplers allow combining real-time systems with passive tuners, without losing high-reflection-coefficient capabilities [11].

In Section III, we will show that these devices are actually "transparent" from 800 MHz up to 15 GHz so that the maximum reflection coefficient at the DUT reference plane is limited only by the probe and short-cable losses. Some measurements performed on a 30-W laterally diffused MOS (LDMOS) device are shown, as an example of the use of passive tuners, in combination with real-time load-pull systems.

Moreover, in Section IV, the advantages arising from the combined use of the load-pull head, active loop, and passive tuner are highlighted, with measurements and with very simple calculations. Finally, some conclusions are briefly discussed.

II. New Directional Coupler

The coupling devices used in this work are an evolution of the prototype presented in [12], with sensible improvements in bandwidth, directivity, and losses.

The so-called *load-pull head* is a reflectometer realized by an 11-cm-long dual-directional coupler. A picture of the device is shown in Fig. 2. It has -26-dB coupling (± 1.5 dB ripple) over the 0.8–18-GHz band. Some other performances are summarized in Table I, whereas directivity and insertion losses are plotted in Fig. 3. These data, along with further experimental verifications, point to the conclusion that the load-pull head's main limitation consists of the directivity, making the device

Manuscript received January 7, 2008; revised May 5, 2008. First published June 13, 2008; current version published October 10, 2008.

The authors are with the Department of Electronics, Politecnico di Torino, 10129 Torino, Italy.

Digital Object Identifier 10.1109/TIM.2008.926044

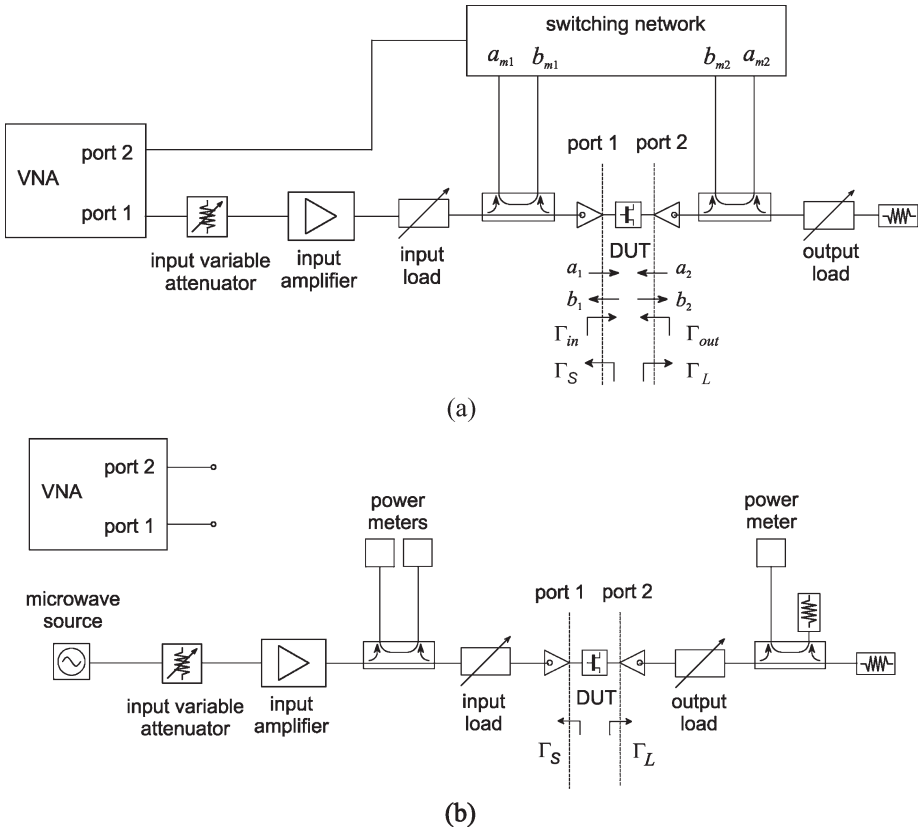

Fig. 1. Simplified scheme of (a) a network-analyzer-based real-time load-pull system and (b) a nonreal-time precalibrated load-pull system.

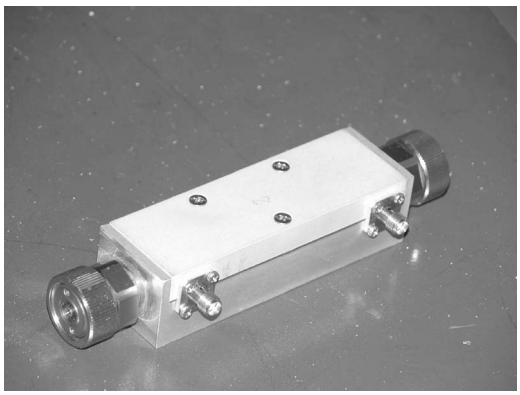

Fig. 2. Picture of the *load-pull head*.

TABLE I
MAIN PERFORMANCES OF THE NEW LOAD-PULL HEAD

Performance	*Value*	*Frequency range*
main line return loss	$<$ - 20 dB	0.8-15 GHz
main line ins loss	$<$ **0.2 dB**	**0.8-15 GHz**
coupled line return loss	$<$ - 20 dB	0.8-15 GHz
coupling	-26 dB $\pm$ 1.5 dB	0.8-18 GHz
directivity	$>$ 10 dB	0.8-13 GHz

usable up to 15 GHz, whereas insertion losses are no longer an issue (up to 18 GHz).

As a comparison, the measured insertion loss of two cascaded commercial stripline directional couplers, in the band 0.8–18 GHz, can be about -0.8 dB at 2 GHz and less than -2.5 dB at 12 GHz, i.e., much worse than the load-pull head.

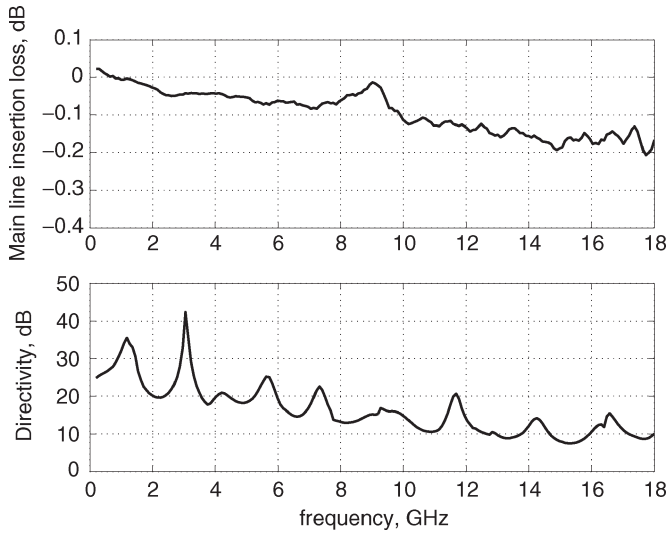

Fig. 3. Load-pull head's main line insertion loss and directivity.

III. PASSIVE REAL-TIME LOAD-PULL SYSTEMS

If we use a load-pull head in a real-time system configuration [Fig. 1(a)], the DUT will see a reflection coefficient that has almost the same magnitude as the one imposed by the load tuning device alone.

To quantify this statement, note that a -0.8-dB loss, which is typical for two cascaded commercial couplers at 2 GHz, transforms an ideal $|\Gamma| = 1$ into a $|\Gamma| = 0.83$ at the DUT reference plane, whereas a -0.05-dB loss, which is a typical

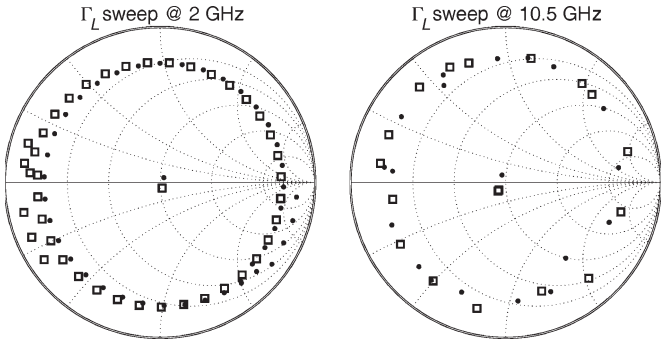

Fig. 4. Γ_L sweep performed with an automatic passive tuner at 2 GHz and at 10.5 GHz. Squares refer to a sweep performed without any device inserted between the reference plane and the tuner, except for a coplanar probe and a short cable. Dots refer to the same sweep performed with a load-pull head inserted between the reference plane and the tuner plus the same coplanar probe and a short cable.

value for a load-pull head at 2 GHz, translates into a $|\Gamma|$ of 0.99 seen by the DUT.

As a further comparison, a -2.6-dB loss corresponds to a $|\Gamma|$ of 0.55, whereas a -0.2-dB loss translates into a $|\Gamma|$ of 0.96 seen by the DUT.

Thus, the load-pull head is nearly transparent up to 15 GHz and, consequently, can be used to extend all the advantages of any real-time system to a passive-tuner-based system. Some of these advantages are the following:

- improved measurement accuracy;
- no need for time-consuming precalibration;
- no need for relying on tuner repeatability;
- real-time monitoring of the all performances.

An experimental verification has been made (see Fig. 4). The same load sweep is performed in two conditions: 1) with the probe directly connected to the tuner (squares) and 2) with the load-pull head inserted between them (dots). Differences between the two conditions are minimal.

A. Application Example: 30-W LDMOS Load-Pull Measurements

As an example application, a high-power (30-W) LDMOS device has been measured at 1.75 GHz with a real-time load-pull test set using passive tuners and load-pull heads, as shown in Fig. 1(a).

The very low input and output impedances of the DUT (in the 5–6-Ω range) give rise to additional issues. To further improve the accuracy and the reachable gammas, the DUT is embedded in a fixture that realizes 50–10-Ω impedance transformation [13]. Calibration standards are also embedded in similar fixtures so that the reference planes are moved to the DUT input and output with a thru-reflect-line calibration. The DUT and standard test fixtures are shown in Fig. 5.

A Γ_L sweep has been performed, with a fixed bias point ($V_{DS} = 28$ V, $V_{GS} = 4$ V, and $I_{DS} = 140$ mA). Results are shown in Fig. 6. The Smith chart is referred to a 10-Ω impedance. Note that during the sweep, a maximum $\Gamma_L = 0.9$, -168° (referred to a 50-Ω impedance) is reached at the DUT reference planes. This maximum gamma corresponds to an

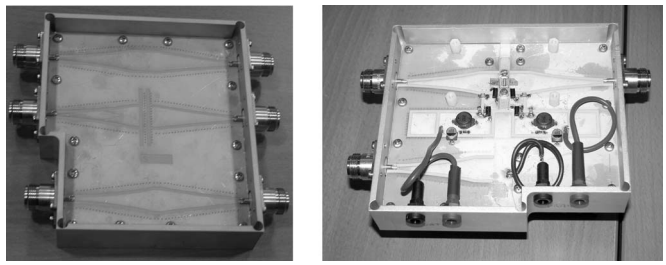

Fig. 5. (Left) Standard and (right) DUT fixtures, used, respectively, for calibration and measurements of a 30-W LDMOS.

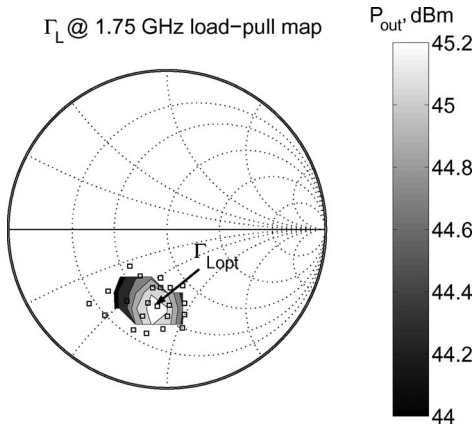

Fig. 6. $P_{\rm out}$ at a 4-dB compression load-pull map of a 30-W LDMOS device at 1.75 GHz. The Smith chart is referred to a 10-Ω impedance.

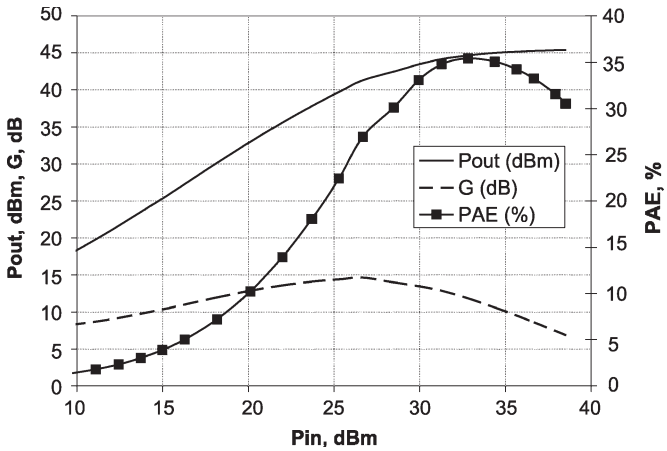

Fig. 7. Power sweep on $Z_{Lopt} = 5.6 - j7.2\ \Omega$.

impedance of $Z_L = 2.7 - j5.2\ \Omega$. This was possible due to the use of the low-loss heads, which are almost transparent at that frequency, i.e., the reflection coefficient presented by the tuner is not diminished by the head losses.

The optimum Γ_L for output power at 4-dB compression is $\Gamma_{Lopt} = 0.8$, -163° (referred to a 50-Ω impedance), corresponding to an impedance of $Z_{Lopt} = 5.6 - j7.2\ \Omega$. A power sweep on this optimum point is shown in Fig. 7. A $P_{\rm out}$ of 45 dBm, with 35% PAE, is reached at 3-dB compression level. Such a high power level is handled with no problem by the low-loss heads, since their main line is an air line [12].

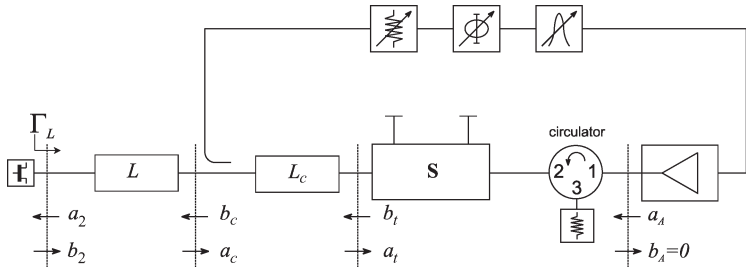

Fig. 8. Active loop architecture.

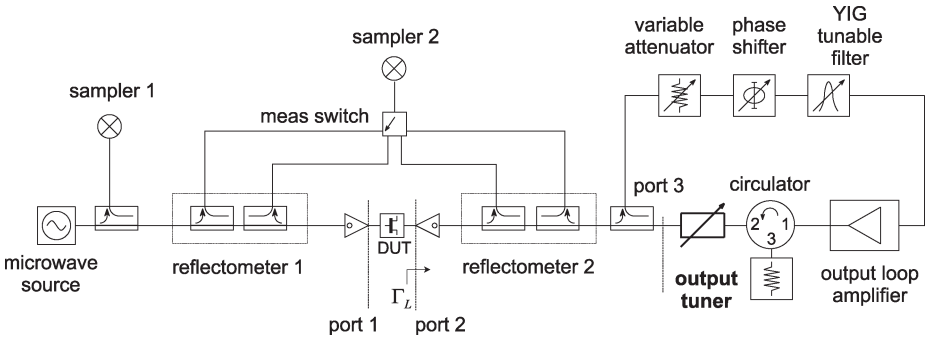

Fig. 9. Simplified scheme of a network-analyzer-based load-pull system combining passive tuning and an active loop.

IV. Load-Pull Head and Active Loop

Let us now consider the active loop architecture in Fig. 8, where Γ_L is the reflection coefficient seen by the DUT. The active loop concept was introduced in 1982 in [14]. A directional coupler placed at the output of the DUT (the *loop coupler*) takes part of the signal and sends it to a variable attenuator, a phase shifter, an yttrium iron garnet filter, and, finally, an amplifier. Then, the signal is reinjected back to the DUT output. Note that the reflection coefficient provided to the DUT does not change with output power if the loop amplifier is in the linear region and has constant gain. Furthermore, note that the use of a circulator is recommended to protect the loop amplifier. In Fig. 8, the unavoidable losses due to cables and probes, which are denoted L and L_c, are also sketched.

In particular, the impact of the losses between the DUT and the loop coupler (L) is twofold: They raise the risk of oscillations [15] and increase the loop amplifier output power needed to synthesize a given Γ_L. When combined with active loops, load-pull heads help reduce both the risk of oscillations and the loop amplifier output power.

A further improvement is given by the combination of an active loop, a passive tuner, and load-pull heads in the configuration shown in Fig. 9.

The passive tuner is a traditional two-port slug tuner (with one or more slugs) placed at the DUT output inside the active loop. Its purpose is to provide pretuning, thus reducing the power needed by the loop amplifier. When the slugs are completely raised up, the tuner does not provide any contributions to Γ_L, which is set by the only active loop. Under this condition, the power provided by the loop amplifier is maximum. On the other hand, when the slugs are fully inserted, the loop is (ideally) cut off, and the loop amplifier does not contribute to Γ_L, regardless of its output power. As a conclusion, between these two extreme cases, there must be an optimal situation (i.e., an optimal tuner slug setting), where the loop amplifier output power has a minimum.

The problem can be approached with a simplified analysis, starting from the loop scheme in Fig. 8. In this scheme, a_2 and b_2 are the waves at the DUT output reference plane, and L and L_c are the losses due to probes, cables, and coupling devices, under the simplified assumption that all these components are perfectly matched. $\mathbf{S}$ is the scattering matrix (S-matrix) of the passive tuner, a_A and b_A are the waves at the output amplifier reference plane, and G is the overall loop gain (including the loop coupler coupling factor, amplifier gain, and overall loop losses). The circulator will be considered ideal; thus, $b_A = 0$.

We define the following quantities.

- Γ_{Lo} is the desired (target) reflection coefficient seen by the DUT (i.e., the reflection coefficient we want to synthesize).
- Γ_{Lt} is the maximum reflection coefficient seen by the DUT, provided by the only passive tuner when the active loop is completely shut down (i.e., $a_A = 0$).

The output amplifier provides a power $P_A = |a_A|^2$, where

$$a_A = G \cdot a_c = G \cdot L \cdot b_2 \tag{1}$$

so we can write

$$P_A = |G|^2 \cdot |L|^2 \cdot |b_2|^2. \tag{2}$$

From the definition of output power P_{out}, when $\Gamma_L = \Gamma_{Lo}$, we have

$$|b_2|^2 = \frac{P_{out}}{1 - |\Gamma_{Lo}|^2}. \tag{3}$$

By replacing (3) into (2), we get

$$P_A = |G|^2 \cdot |L|^2 \cdot \frac{P_{out}}{1 - |\Gamma_{Lo}|^2}. \tag{4}$$

Moreover, by introducing the S_{ij} $(i, j = 1, 2)$ elements of the tuner S-matrix, we can write

$$b_t = S_{11} a_t + S_{12} a_A. \tag{5}$$

We now make the following assumptions, which are valid for low (i.e., < -20 dB) coupling of the loop coupler:

$$\begin{aligned} b_t &= \frac{a_2}{LL_c} \\ a_t &= LL_c b_2 \end{aligned} \tag{6}$$

and substitute (6) and (1) into (5):

$$\frac{a_2}{LL_c} = S_{11}(LL_c) b_2 + S_{12} G L b_2. \tag{7}$$

From (7), we can compute G:

$$G = \frac{\Gamma_{Lo} - S_{11}(LL_c)^2}{S_{12} L (LL_c)}. \tag{8}$$

In our case, S_{11} and S_{12} are not completely independent. For a lossless reciprocal tuner, it holds that

$$|S_{11}|^2 + |S_{21}|^2 = |S_{11}|^2 + |S_{12}|^2 = 1. \tag{9}$$

In case of low tuner losses, we can make the simplified assumption that

$$|S_{11}|^2 + |S_{12}|^2 = |\gamma|^2 \tag{10}$$

where $|\gamma|$ is the maximum value that $|S_{11}|$ can reach.

From (4), (8), and (10), we get

$$P_A = \frac{\left|\Gamma_{Lo} - S_{11}(LL_c)^2\right|^2}{\left(|\gamma|^2 - |S_{11}|^2\right) |LL_c|^2} \frac{P_{\text{out}}}{1 - |\Gamma_{Lo}|^2}. \tag{11}$$

Equation (11) gives some highlights on the behavior of the amplifier output power, with respect to Γ_{Lo}, S_{11}, and overall losses LL_c. It is somewhat similar to [13, eq. (5)] but is valid for a general tuning device, and it is now possible to make further considerations on the optimization of the tuner settings.

For simplicity, let us consider a case where S_{11} and Γ_{Lo} are purely real and S_{11} can continuously vary between zero and γ. For a fixed desired Γ_{Lo} value, we can plot P_A versus S_{11}. In Fig. 10, we have chosen $\Gamma_{Lo} = 0.96$ and $\gamma = 1$ and plotted P_A for several values of LL_c, from -2.4 dB (typical for commercial couplers) to -0.4 dB (obtainable with load-pull heads). Note that in this picture, P_A is normalized with respect to its value corresponding to $LL_c = -2.4$ dB and $S_{11} = 0$.

First, this picture shows the advantage of using a load-pull head as a loop coupler in an active loop. It reduces the requirements on loop amplifier output power by reducing the attenuation term LL_c. For $S_{11} = 0$ (i.e., the tuner is not present or behaving like a matched transmission line), the required P_A to obtain $\Gamma_{Lo} = 0.96$ is 2 dB lower for

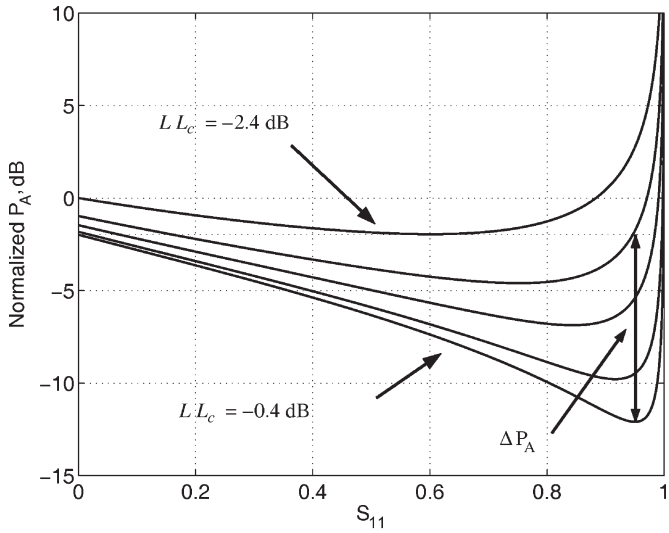

Fig. 10. Normalized loop amplifier output power P_A versus tuner S_{11} for different values of overall losses. ΔP_A is the difference between the minimum P_A and its value for $S_{11} = 0$.

$LL_c = -0.4$ dB, with respect to the value of the required power when $LL_c = -2.4$ dB.

Furthermore, this picture clearly shows the effects of using a tuner as a prematching device in an active loop. Indeed, the minimum required amplifier power as a function of the tuner S_{11} strongly depends on the overall losses. Calling ΔP_A the difference between the minimum P_A and its value for $S_{11} = 0$, as sketched in the picture, we have a ΔP_A of 2 dB for -2.4-dB losses and of 10 dB for -0.4-dB losses. This is clearly an advantage of using load-pull heads with an active loop combined with a passive tuner.

By zeroing the first derivative of (11) on the real axis, we find that one of the minimum values for P_A corresponds to

$$S_{11\,\min} = \frac{\gamma^2 (LL_c)^2}{\Gamma_{Lo}}. \tag{12}$$

If the active loop is shut down, i.e., $a_A = 0$, and the tuner S_{11} is set to this value, the reflection coefficient seen at the Γ_L reference plane will be

$$\Gamma_{L\,\min} = \frac{\gamma^2 (LL_c)^4}{\Gamma_{Lo}}. \tag{13}$$

Note that when $a_A = 0$, the maximum $|\Gamma_L|$ obtainable with the tuner is

$$|\Gamma_{Lt}| = |\gamma| (LL_c)^2. \tag{14}$$

This means that setting the tuner to $|S_{11min}|$ corresponds to having a reflection coefficient magnitude at the DUT reference plane of

$$|\Gamma_L| = \frac{|\Gamma_{Lt}|^2}{|\Gamma_{Lo}|}. \tag{15}$$

With these considerations, a practical procedure to find the best tuner position (i.e., the one that minimizes the amplifier

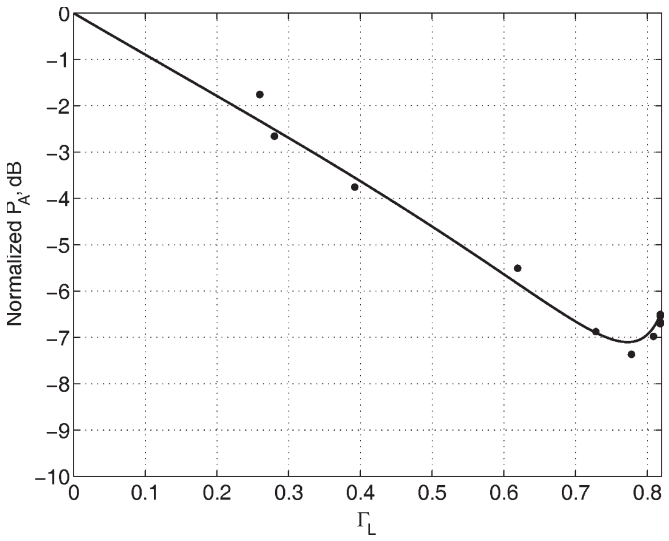

Fig. 11. Measured and simulated normalized P_A versus Γ_L and the reflection coefficient (real) seen at the DUT output when the loop is shut down. A fixed reflection coefficient of 0.96 was chosen as the desired Γ_{Lo}. Measurements are performed under continuous-wave conditions at 4 GHz.

power) and to obtain the desired Γ_{Lo} is the following.

- Measure the maximum $|\Gamma_{Lt}|$ obtainable with the tuner when the loop is shut down.
- If the desired $|\Gamma_{Lo}| < |\Gamma_{Lt}|$, there is no need for active load pull.
- Otherwise, set the tuner when the loop is shut down, so that $|\Gamma_L| = (|\Gamma_{Lt}|^2/|\Gamma_{Lo}|)$ and $\angle\Gamma_L = \angle\Gamma_{Lo}$; this corresponds to setting the S_{11} of the tuner equal to the $S_{11\,\min}$ of (12).
- Finally, synthesize the desired Γ_{Lo} by properly setting the active-loop attenuator and phase shifter.

This procedure has been applied to a real-time load-pull test bench while monitoring the amplifier output power P_A with a power meter. A real reflection coefficient of 0.96 was chosen as the desired Γ_{Lo}. The maximum (real) Γ_{Lt} obtainable with the tuner was in our case 0.86. The estimated best tuner position is then 0.77.

In Fig. 11, P_A (measured and simulated) is normalized and plotted versus the Γ_L of the tuner alone, which is seen at the DUT reference plane.

These results confirm that the loop amplifier output power reaches the minimum value for $\Gamma_L = 0.77$, as predicted by the simplified theory. In conclusion, combining load-pull heads, tuner, and active loop sensibly reduces the loop amplifier cost, as its output power sensibly drops.

V. Conclusion

Some recent advances in real-time load-pull technologies have been described. A recently introduced directional coupler, i.e., the ultralow-loss load-pull head, can transform any passive precalibrated load-pull system into a real-time load-pull test set, without losing high-reflection-coefficient capabilities. For the first time, the load-pull head was implied in a real-time passive load-pull test bench, and measurements give evidence that it is nearly "transparent" up to 15 GHz and capable of handling very high power. The new head can also be used to reduce the risk of oscillations and the loop amplifier output power in active loop architectures. Finally, some additional advice to bypass the remaining unavoidable losses due to probes and cables was given. The joint use of load-pull heads, a passive tuner, and an active loop not only boosts the available Γ_L but also decreases the loop amplifier output power, with a sensible reduction in the overall cost of the system.

References

[1] G. Heiter, "Characterization of nonlinearities in microwave devices and systems," *IEEE Trans. Microw. Theory Tech.*, vol. MTT-21, no. 12, pp. 797–805, Dec. 1973.

[2] J. Cusack, S. Perlow, and B. Perlman, "Automatic load contour mapping for microwave power transistors," *IEEE Trans. Microw. Theory Tech.*, vol. MTT-22, no. 12, pp. 1146–1152, Dec. 1974.

[3] B. Bianco, M. Parodi, S. Ridella, and F. Selvaggi, "Launcher and microstrip characterization," *IEEE Trans. Instrum. Meas.*, vol. IM-25, no. 4, pp. 320–323, Dec. 1976.

[4] J. Jargon, R. Marks, and D. Rytting, "Robust SOLT and alternative calibrations for four-sampler vector network analyzers," *IEEE Trans. Microw. Theory Tech.*, vol. 47, no. 10, pp. 2008–2013, Oct. 1999.

[5] A. Ferrero and U. Pisani, "QSOLT: A new fast calibration algorithm for two-port s-parameter measurements," in *38th ARFTG Conf. Dig.*, San Diego, CA, Dec. 1991, pp. 15–24.

[6] A. Ferrero and U. Pisani, "Two-port network analyzer calibration using an unknown 'thru'," *IEEE Microw. Guided Wave Lett.*, vol. 2, no. 12, pp. 505–507, Dec. 1992.

[7] R. Tucker and P. Bradley, "Computer-aided error correction of large-signal load-pull measurements," *IEEE Trans. Microw. Theory Tech.*, vol. MTT-32, no. 3, pp. 296–300, Mar. 1984.

[8] I. Hecht, "Improved error-correction technique for large-signal load-pull measurements," *IEEE Trans. Microw. Theory Tech.*, vol. MTT-35, no. 11, pp. 1060–1062, Nov. 1987.

[9] A. Ferrero and U. Pisani, "An improved calibration technique for on-wafer large-signal transistor characterization," *IEEE Trans. Instrum. Meas.*, vol. 47, no. 2, pp. 360–364, Apr. 1993.

[10] V. Teppati and A. Ferrero, "New perspectives in non linear device and amplifier characterization," in *Proc. GAAS Conf.*, Milan, Italy, Sep. 2002.

[11] A. Ferrero, V. Teppati, and U. Pisani, "Recent improvements in real-time load-pull systems," in *Proc. Instrum. Meas. Technol. Conf.*, Sorrento, Italy, Apr. 24–27, 2006, pp. 448–451.

[12] V. Teppati and A. Ferrero, "A new class of nonuniform, broadband, nonsymmetrical rectangular coaxial-to-microstrip directional couplers for high power applications," *IEEE Microw. Wireless Compon. Lett.*, vol. 13, no. 4, pp. 152–154, Apr. 2003.

[13] Z. Aboush, J. Lees, J. Benedikt, and P. Tasker, "Active harmonic load-pull system for characterizing highly mismatched high power transistors," in *IEEE MTT-S Symp. Tech. Dig.*, Long Beach, CA, Jun. 12–17, 2005, pp. 1311–1314.

[14] G. P. Bava, U. Pisani, and V. Pozzolo, "Active load technique for load-pull characterization at microwave frequencies," *Electron. Lett.*, vol. 18, no. 4, pp. 178–179, Feb. 1982.

[15] A. Ferrero, "Active load or source impedance synthesis apparatus for measurement test set of microwave components and systems," U.S. Patent 6 509 743, Jan. 21, 2003.

Valeria Teppati (S'00–M'04) was born in Torino, Italy, on October 20, 1974. She received the Laurea degree in electronic engineering and the Ph.D. degree in electronic instrumentation from the Politecnico di Torino in 1999 and 2003, respectively.

In 2003, she joined the Department of Electronics, Politecnico di Torino, as a Research and Teaching Assistant. She has been an Assistant Professor at Politecnico di Torino since 2005. Her research interests and activities include microwave device design, linear and nonlinear measurement design, multiports, calibration, and uncertainty.

Andrea Ferrero (S'86–M'88) was born in Novara, Italy, on November 7, 1962. He received the Laurea degree in electronic engineering and the Ph.D. degree in electronics from the Politecnico di Torino, Torino, Italy, in 1987 and 1992, respectively.

In 1988, he joined the Aeritalia Company as a Microwave Consultant. He was with the Microwave Technology Division, Hewlett-Packard, Santa Rosa, CA, as a Summer Student in 1991. He was with the Department of Electrical Engineering, Ecole Polytechnique de Montréal, Montréal, QC, Canada, as a Guest Researcher in 1995. He became an Associate and Full Professor of electronic measurements with the Department of Electronics, Politecnico di Torino, in 1998 and 2006, respectively. His main research activities are in the areas of microwave measurement techniques, calibration, and modeling.

Dr. Ferrero received the Automatic RF Techniques Group Technology Award for the development and implementation of vector network analyzer calibration algorithms and nonlinear measurement techniques in 2006.

Umberto Pisani received the Dr.Ing. degree in electronic engineering from the Politecnico di Torino, Torino, Italy, in 1967.

In 1968, he joined the Department of Electronics, Politecnico di Torino, as an Assistant Professor. In 1982, he became an Associate Professor and, in 1989, a Full Professor of electronics. He has conducted research in the area of active and passive device characterization and modeling, mainly of microwaves. In this field, he contributed to the development of experimental techniques, concerning both bipolar transistors and MESFETs, in linear and large-signal behavior in the design of solid-state broadband amplifiers and power stages for satellite applications.